# PARAMETRIC STUDY OF THE DYNAMIC ALONG-WIND RESPONSE OF A GUYED TOWER

**Jorge S. Ballaben**[a,b] **and Marta B. Rosales**[a,b]

[a]*Departamento de Ingeniería, Universidad Nacional del Sur, Av. Alem 1253, (8000) Bahía Blanca, Argentina, jorgeballaben@gmail.com,mrosales@criba.edu.ar*

[b]*CONICET, Argentina*

**Keywords:** Guyed tower, guy tension, dynamic response, wind.

**Abstract.** As wireless communications spread, there is an increasing demand for antenna supporting structures. Lattice towers are commonly used systems, either self-supported or guyed. The latter are chosen for economical reasons when there is enough space for their location. Radio and television employ structures that range between 100 and 600 m and communication towers for mobile phones are around 60 m though higher structures are also constructed. For large heights, guyed masts are indicated. However, it depends on the customer preferences, suppliers, budget and location. Generally, self-supported structures are preferred in urban areas and guyed masts in the countryside. Nowadays the demand for more accurate and reliable communication systems poses higher structural demands since the signal technology sometimes requires of very small motions of the supporting structures to achieve a high quality transmission. The design of these structures is, in general, carried out following the standard codes and simplified models. The dynamic actions, as wind and earthquakes, are not addressed in detail with exception of special cases, despite the large potential of adverse impact. Guyed structures stiffness are highly dependent on the guys tension. The influence of this parameter is relevant to the dynamic response. Also, the mast stiffness and damping are variables of interest. In this work, the dynamic response of a communication lattice guyed tower is analyzed under wind loads and the degree of influence of the mentioned parameters is assessed. The mean wind load is derived from the standard's approach while the fluctuating wind component is obtained through the Spectral Representation Method (SRM). The algorithm starts from a given Power Spectral Density (PSD). The temporal and spatial correlations are taken into account by finding the cross-spectrum and introducing a coherence function. The method yields a temporal record of the fluctuating wind velocity for each desired height of the tower. It is possible to show that the wind velocity thus found can reproduce the starting point PSD. Once the wind velocity is introduced in the wind pressure expression of the standard code CIRSOC-INTI (2005), the fluctuating loads are derived for the mast. A finite element discretization is employed with these loads using an equivalent beam model for the lattice tower and truss elements with pretension for the cables (guys). A standard case with fixed values of guy tensions, tower stiffness and damping is first considered. Then, the three parameters are varied within practical ranges. Some outcomes of the dynamic response are analyzed, e.g. mean, minimum and maximum values of the top displacement of the tower and the dynamic tension of the cables. Several plots are derived to stress the influence of the parameters. Results are compared with a previous study in which a fully correlated load was assumed, i.e. the wind velocity was generated as a combination of harmonic deterministic functions.

Figure 1: Typical guyed tower for mobile signal transmission.

# 1   INTRODUCTION

For many years, guyed masts have been used to support antennas for radio, TV and other types of communication (Fig. 1. This structure has clear advantages in the open country, where there are no restrictions on the position of the cable anchors. However, this kind of structures is, sometimes, also found in urban areas, due to its low cost, compared with other typologies. A typical configuration comprises a lattice tower with triangular cross-section (three legs, horizontal and diagonal members) (see Fig. 1). The height is variable depending on the functions, but nowadays is not exceptional to see 300 m-height towers. The main structural characteristics are the large slenderness of the mast and several levels of taut guys. Dynamic loads as wind, are usually simplified as quasistatic loads that represents the mean of the dynamic phenomena amplified with factors that account for the dynamics characteristics at each case, following standard codes and recommendations. Wind load contains energy that interacts with flexible structures. Hence the dynamic response becomes important in the analysis of guyed masts. The mast acts strongly in a non-linear fashion when the guys vary between a slack and a taut state.

Research on this subject includes works by Kahla (1993) who employs equivalent beam methods in order to simplify five lattice mast and carries out statics analysis. Wahba et al. (1998) and Wahba and Monforton (1998) evaluate the behavior of guyed towers, modeling the mast as a lattice truss beam or with beam elements. The finite elements procedure is used to model six existing guyed masts, in order to study the influence of guy initial tensions and torsion resistors on the dynamic response of the structure. A hybrid model is proposed by Kewaisy (2001) that includes non-linear considerations, modeling the guys with a finite difference approximation and the mast with finite elements. The response of a guyed mast to a guy rupture under no wind pressure is analyzed by Kahla (2000), using a program developed by the author. Punde (2001) studies dynamics of cable supported structures using a generalized finite element approach. The non linear spectral element method in order to analyze the non linear dynamic response of a guyed mast is used by Horr (2004). The dynamic response of guyed masts using different models for cables and evaluates the variation of the stiffness of the complete system using different levels of pre-stress on guys is compared by Preidikman et al. (2006). Meshmesha

et al. (2006) introduce an equivalent beam-column analysis based on an equivalent thin plate approach for lattice structures, then evaluates the accuracy of the proposed method and classic methods to determine the equivalent beam properties (the unit load method and the energy approach are employed) in determining the response of a guyed tower subjected to static and seismic loading. The finite elements approach was also used by Shi (2007) and de Oliveira et al. (2007). Lu et al. (2010) introduce the principle of harmonic wave superimpose method for wind velocity simulation, as well as the improved method by introducing FFT in harmonic superimpose wave method. Wind velocity time series along the height of guyed-mast was simulated with the improved method. Regarding codification issues, Matuszkiewicz (2011) evaluates selected problems concerning designing of guyed masts with lattice shaft in accordance with the "EN 1993-3-1: Design of steel structures. Part 3-1: Towers, masts and chimneys-Towers and masts" and discusses the method of application of the mast shaft geometrical imperfections in the calculation.

In this work, a simplified model of a 120 m guyed tower is studied. Its dynamic response, under the action of wind loads, with five different pre-stress on the cables, three values of tower stiffness and three values of damping, is tackled through a finite element procedure. The lattice mast is modeled through an equivalent beam-column. Then, the finite element model of the mast is made of two-node beam elements and is supposed fixed at the base. Four levels of cables are modeled with truss elements considering the lack of compression capability of the cables. To account for the intrinsic nonlinear behavior of this structural system, the analysis is carried out with a mechanical event simulation modulus of the finite element package ALGOR (2009) for wind studies.

The gravity loads on the tower and cables and the initial pre-stressing of the cables first are applied until the model attains static equilibrium (avoiding the transient perturbation). Then the dynamic wind load is activated. The wind real velocity field is reproduced through the Spectral Representation Method, presented in Shinozuka and Jan (1972), using the power spectral density function proposed by Davenport (see for instance, Dyrbye and Hansen (1994)).

The results are referenced to a previous work of the authors Ballaben et al. (2011) where the dynamics of the wind load were approximately modeled as a superposition of cosine functions, with frequencies within the peak zone of the same power spectral density function used in here, thus assuming fully correlated loads. The results obtained by the two approaches are then compared.

## 2 FINITE ELEMENT MODEL FOR GUYED TOWER

The finite element model considered herein, is similar to that used by Punde (2001). The three dimensional guyed tower is 120 m high and has four guy levels separated by 30 m, with three guys at each level, oriented in vertical planes separated by 120°, and two sets of guy anchors in each of the three planes (see Fig. 2).

To construct the model, the finite element software ALGOR (2009) was used. The tower (mast) is modeled as a beam-column, made of twelve 6-DOF beam elements and fixed at the base. Each guy is modeled using twenty 3-DOF two-node pre-stressed truss elements. Both element types allows large displacement.

The mast weight per unit length is 61 kg/m, the modulus of elasticity is 209 GPa, the cross-sectional area is 0.00198 $m^2$ and the reference second area moment in any direction is 0.0018 $m^4$. The guy cross-sectional area is 0.0002 $m^2$, the modulus of elasticity is 150 GPa, the weight per unit length is 2.55 kg/m and the reference case pretension is 25 kN.
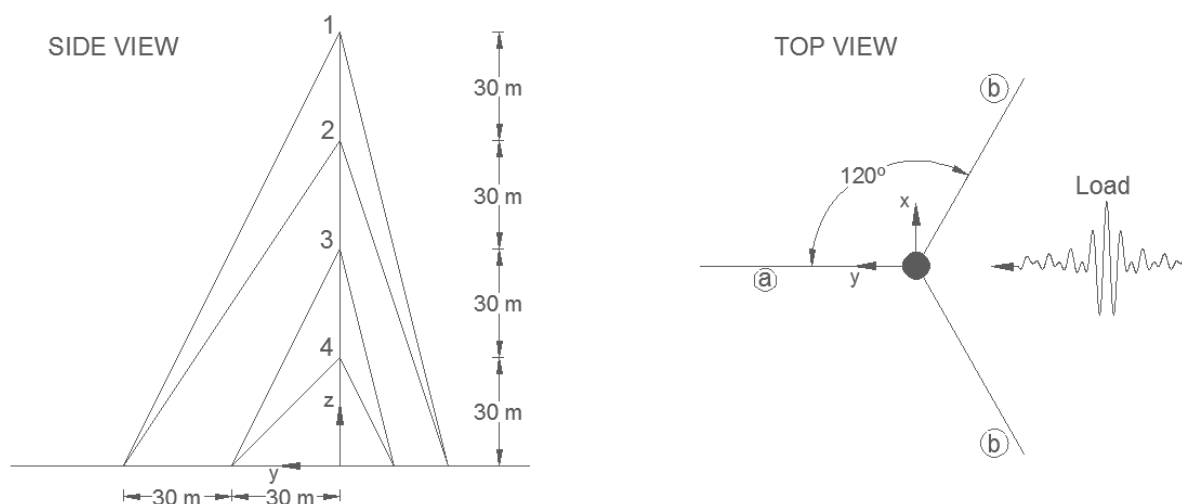
Figure 2: Guyed mast geometry.

## 3 SENSITIVITY STUDIES

At the design stage or the retrofitting of guyed towers is evaluated, uncertainties on some parameters of the dynamic problem are commonly found as: i) the initial pretension of the guys, ii) the equivalent damping (Rayleigh) of the structure and iii) the stiffness of the mast, are commonly found. This is the motivation to carry out a sensitivity study in order to measure the influence of those parameters on the dynamic response.

### 3.1 Initial pretension of the guys

The initial guy pretension is the tensile force that is needed to ensure the stability of the structural system. For design purposes the ANSI/TIA-222-G (2009) sets a range of 7-15% of the ultimate strength of the guy.

Due the lack of suitable measuring devices for the initial pretension of the guys, in several opportunities the initial pretension does not match the expected value and can even be out of the recommended range.

This work is intended to cover the range proposed for the standards. Based on the cross section and material of the guys, were used the following values of initial pretension: 15, 20, 25, 30, 35 kN.

### 3.2 Equivalent damping of the structure

The Rayleigh damping is proportional to the mass matrix and the stiffness matrix, and allows the decoupling of the damping matrix. The inclusion of damping is necessary to model the real dissipation of the vibrations. Gomathinayagam and Lakshmanan (2003) found from experimental measures on a lattice guyed mast, values in the range of 1-3% of the critical damping. On the other hand the IASS (1991) standard recommends using 3% for bolted unions, the CIRSOC-INTI (2008) the 2% and the ANSI/TIA-222-G (2009) the 5% for seismic temporal analysis. This review of the state of the art show that the recommended range is 1-5% of the critical damping for this type of structures. In this paper, three cases for the Rayleigh damping are considered: 1%, 2% and 3% of the critical damping. The proportional coefficients for the mass and stiffness matrix were 0.118 and 0.00070, 0.237 and 0.00144, y 0.356 and 0.00209, respectively.

These coefficients correspond to the standard case and are used in all cases due to the minor variations that exist for other combinations of parameters.

## 3.3 Bending stiffness of the mast

The bending stiffness of the mast (proportional to the second area moment of the cross section of the mast) is determined on the design stage. However, the reinforcement (due to the need to change or incorporate new equipment) is nowadays a common practice. This improvement introduces changes on the designed value of the second area moment that affects the behavior of the structure.

In this work, the following values were used: $1.80 \times 10^{-3}$, $2.25 \times 10^{-3}$ and $2.70 \times 10^{-3}$ m$^4$.

## 4 LOADS

In order to simulate typical load conditions, three loads were taken into account: weight (gravitational load), pre-stress on the cables and wind loads in the $y$ direction (which defines an axis of symmetry in the arrangement of cables, see Fig. 2). Only displacements on the $y$ direction will be reported. At this stage no other loads, like wind, isolators, etc., are applied on the guys.

### 4.1 Wind Load Design

The method used in this work, in order to simulate a wind load, was the Spectral Representation Method (SRM) first proposed by Shinozuka and Jan (1972), and then implemented by several authors.

The method starts from a power density function and a coherence function, to be chosen according the type of problem to be simulated. Then, the random signals are created as a superposition of harmonic functions with a random phase angle, weighed by coefficients that represent the importance of the value of frequency within the spectrum and the spatial correlation. The power density function is discretized in regular intervals and the frequencies used in the harmonic functions are chosen randomly within each interval, in order to avoid a harmonic result. In the following, the method will be introduced theoretically and then the implementation will be described. The power density function employed was the proposed for Davenport, and can be found, for instance, in Dyrbye and Hansen (1994). The velocity height variation was taken from the Argentinian standards CIRSOC-INTI (2005).

#### 4.1.1 Spectral Representation Method

Following the methodology developed in Shinozuka and Jan (1972), let us first consider a set of $m$ gaussian stationary random processes $f_j^0(t), j = 1, 2, \ldots, m$, with zero mean, $E[f_j^0(t)] = 0$, with a cross spectral density matrix $S^0(w)$ given by

$$S^0(w) = \begin{bmatrix} S_{11}^0(w) & S_{12}^0(w) & \cdots & S_{1m}^0(w) \\ S_{21}^0(w) & S_{22}^0(w) & \cdots & S_{2m}^0(w) \\ \vdots & \vdots & \ddots & \vdots \\ S_{m1}^0(w) & S_{m2}^0(w) & \cdots & S_{mm}^0(w) \end{bmatrix}, 0 \leq w \leq \infty$$

where $S_{jk}^0(w) = F[R_{jk(\tau)}^0]$. $F[\ ]$ represents the Fourier Transform operator and $R_{jk}^0(\tau)$ is the cross-correlation function $(j \neq k)$ or the autocorrelation function $(j = k)$. This matrix verifies $S_{jk}^0(w) = \bar{S}_{jk}^0(w)$ because for stationary processes the correlations matrix verifies $R_{jk}^0(\tau) =$

$R^0_{jk}(-\tau)$ and then $S^0(w)$ is Hermitian and definite positive matrix. If the lower triangular matrix $H(w)$ is defined as a matrix whose Fourier transform exists, the relationship is

$$S^0(w) = H(w)\bar{H}^T(w) \tag{1}$$

where the bar stands for complex conjugate and the superscript $T$ its transpose. The $f^0_j(t)$ process can be simulated by the following series (Shinozuka and Jan, 1972):

$$f_j(t) = \sum_{k=1}^{m} \sum_{n=1}^{N} |H_{jk}(w_n)|\sqrt{2\Delta w}\cos[\hat{w}_n t + \theta_{jk}(w_n) + \Phi_{kn}] \tag{2}$$

where $\Delta w$ is the frequency interval with which the power spectrum density function is discretized, $w_n = \Delta w(n-1)$, $\hat{w}_n = w_n + \psi_{kn}\Delta w$, $\psi_{kn}$ is a random value uniformly distributed between $0$ and $1$, $N$ is the amount of frequency ranges, $\Phi_{kn}$ are the random independent phase angles uniformly distributed between $0$ and $2\pi$ and

$$\theta_{jk} = \tan^{-1}\left[\frac{\Im\{H_{jk}(w_n)\}}{\Re\{H_{jk}(w_n)\}}\right]$$

where $\Im\{\}$ and $\Re\{\}$ are the imaginary and real parts, respectively. If the values of $S_{jk}$ are all real, $\theta_{jk}(w_n)$ is equal to zero. In order to find the decomposition represented by Eq. (1), is possible to follow two different paths: the *Cholesky Decomposition* of the spectral density matrix (Shinozuka and Jan, 1972) or the *Modal Decomposition*. It can be proved that the group mean $E[f_j(t)]$ is zero

$$E[f_j(t)] = 0$$

and the cross-correlation $R_{jk}(\tau)$ is given by

$$R_{jp}(\tau) = \sum_{k=1}^{m} \sum_{n=1}^{N} |H_{jk}(w_n)H_{pk}(w_n)|2\Delta w\cos[w_n t - \theta_{pk}(w_n) + \theta_{jk}(w_n)]$$

for $N \to \infty$:

$$
\begin{aligned}
R_{jp}(\tau) &= \lim_{N\to\infty}\sum_{k=1}^{m}\sum_{n=1}^{N} H_{jk}(w_n)\bar{H}_{pk}(w_n)e^{iw_n\tau}\Delta w \\
&= \int_0^\infty \sum_{k=1}^{m} H_{jk}(w_n)\bar{H}_{pk}(w_n)e^{iw_n\tau}dw \\
&= \int_0^\infty S^0_{jp}(w)e^{iw_n\tau}dw \\
&= R^0_{jp}(\tau)
\end{aligned}
$$

Thus, the process $f_j(t), j = 1, 2, ..., m$ simulated by the Eq. (2) produces the desired cross-correlation function, $R^0_{jp}(\tau)$ and spectral density $S^0_{jp}(w)$ with respect to the group mean.

### 4.1.2 Spectral Representation Method (SRM) implementation for the time dependent wind velocity field

In order to model the dynamics of wind, the implementation of the SRM will be next explained step by step. The first step is the adoption of a power spectral density function (*psdf*)

and a coherence function. In this work, the *psdf* suggested for Davenport is used, e.g. reported in Dyrbye and Hansen (1994):

$$R_N(z,w) = \frac{wS(z,w)}{\sigma^2(z)} = 2/3\frac{f_L^2}{(1+f_L^2)^{4/3}} \tag{3}$$

where $w$ is the frequency in $Hz$, $\sigma$ is the standard deviation and $f_L$ is the non-dimensional frequency:

$$f_L = w\frac{L_u}{U(z)} \tag{4}$$

$L_u$ is the length scale of turbulence (for the Davenport model is adopted as 1200 $m$) and $U(z)$ is the height dependent value of wind mean velocity. The expression for $U(z)$ corresponds to the potential law adopted by the Argentinian standard CIRSOC-INTI (2005)

$$U(z) = 2.01V(z/z_g)^{2/\alpha} \tag{5}$$

in which $z$ is the height of the analyzed point, $V$ is the wind velocity and together with $z_g$, and $\alpha$ are values given by the standard for the characteristics of the location zone of the structure and will be further explained in the section 4.1.3. The coherence function is

$$Coh(z_i, z_j, w) = exp\left\{-2w\frac{C_z|z_i - z_j|}{U(z_i) + U(z_j)}\right\} \tag{6}$$

where $z_y$ and $z_j$ are the heights two given points in the mast. Then, each $S_{ij}$ of the $S(w)$ matrix, for a given value of frequency can be calculated as:

$$S_{ij}(z_i, z_j, w) = \sqrt{S(z_i, w)S(z_j, w)}\, Coh(z_i, z_j, w) \tag{7}$$

Following this procedure, N matrices will be created, one for each value of frequency. Next, these matrices will have to be transformed in order to find the $H(w)$ matrices. In this work, the authors used a Matlab command that executes the Cholesky Transform.

Having the $H(w)$ matrices, is possible to construct the temporal series given by

$$u(z_j, t) = \sum_{k=1}^{m}\sum_{n=1}^{N} H_{jk}(w_n)\sqrt{2\Delta w}\cos[2\pi\hat{w}_n t + \Phi_{kn}] \tag{8}$$

Here $H_{jk}(w_n)$ is used instead of $|H_{jk}(w_n)|$ and $\theta_{jk}(w_n)$ is neglected because only the real part of the *psdf* is taken into account. The maximum frequency of the spectrum considered was $w_c = 2.5$ Hz. The frequency interval $\Delta w$ was selected as 0.004 Hz. The time interval required to generate the Eq. (8) is $\Delta t \leq 1/2w_c$. The value adopted in this work is $\Delta t = 0.20\ s$. The height of the mast was discretized in twelve equidistant points. Table 1 summarizes the values of the most relevant parameters in order to apply the method and Fig. 3 shows the matching between the theoretical wind power spectrum with the one obtained from the fourier transform of the cross-correlation function of two signals obtained by the Eq. (8).

Table 1: Coefficients for calculating the time dependent velocity field.

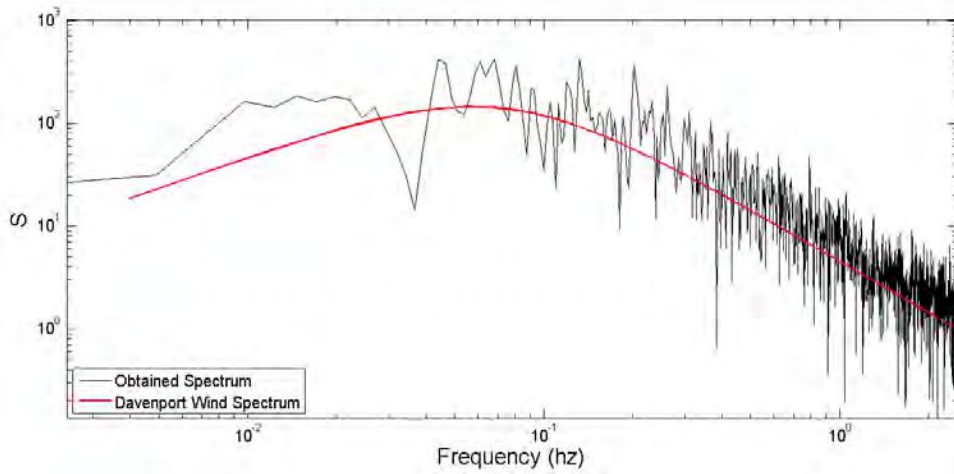| Coefficient | $\sigma^2$ | $L_u$ | $C_z$ | $w_c$ | $\Delta w$ | $\Delta t$ | N | m |
|---|---|---|---|---|---|---|---|---|
| Value | 38.77 | 1200 $m$ | 11.5 | 2.5 $hz$ | 0.004 $hz$ | 0.2 $s$ | 625 | 12 |

Figure 3: Comparison of the wind velocity spectrum of the velocity series with the theoretical expression.

### 4.1.3 Wind Load Construction

In the previous section, the time dependent component of the wind velocity was derived. Next,the procedure to construct the time dependent wind load will be explained. The wind load is calculated following the Argentinian standard code CIRSOC-INTI (2005) that specifies the steps for the construction of a static load. Some modifications are introduced in order to take into account the dynamics of the wind velocity, modeled by the Eq. (8). The standard defines the static wind load as

$$F = q_z * G * C_f * A_f \tag{9}$$

where $F$ is the magnitude of the wind load, $G$ is the gust coefficient, which takes into account the effects of the dynamic amplification (resonance) and lack of correlation of loads, $A_f$ is the exposed area of the mast, projected onto the plane normal to the loads and $C_f$ is a coefficient which takes into account the shape of the structure, in this case, the mast. Its formula is:

$$C_f = 3,4 * \epsilon^2 - 4,7 * \epsilon + 3,4 \tag{10}$$

where $\epsilon = A_f / A_t$ and $A_t$ is the exposed area of the mast without holes. In Eq. (9) $q_z$ is the wind pressure and is formula is:

$$q_z = 0,613 * k_z * k_{zt} * k_d * V^2 * I \tag{11}$$

where $I$ defines the category of the structure, $V$ is the reference velocity, defined at each zone of the country (in this case, Bahía Blanca, Argentina), $k_{zt}$ is the topographic coefficient, $k_d$ is the direction coefficient, that takes into account the type of structure (i.e. lattice towers, buildings, etc.) and $k_z$ is a empirical coefficient that considers the load variation with height and is equation is:

$$k_z = 2.01 * (z/z_g)^{2/\alpha} \tag{12}$$

Here $z$ is the height of the point considered, $z_g$ and $\alpha$ are obtained from code tables. As the term $k_z * V$ was already used in order to create the time dependent component (Eq. (5)), and

describes the velocity for height $z$, it will be replaced for $U(z) + u(z,t)$:

$$\bar{q}_z = 0,613 * k_{zt} * k_d * V * (U(z) + u(z,t)) * I \tag{13}$$

Replacing $q_z$ by $\bar{q}_z$ in Eq. (9) results

$$F(z,t) = \bar{q}_z * G * C_f * A_f \tag{14}$$

Table 2 shows the numerical values adopted and calculated for the coefficients.

Table 2: Coefficients for calculating static wind loads according to CIRSOC-INTI (2005)

| Coefficient | $G$ | $A_f$ | $A_t$ | $C_f$ | $I$ | $V$ | $k_d$ | $k_{zt}$ |
|---|---|---|---|---|---|---|---|---|
| Value | 0.85 | 0.57 m$^2$ | 9.41 m$^2$ | 3.13 | 1.00 | 55 m/s | 0.85 | 1 |

Figure 4 shows the mean load variation with altitude on the mast and Fig. 5 illustrates the shape of the obtained wind load.
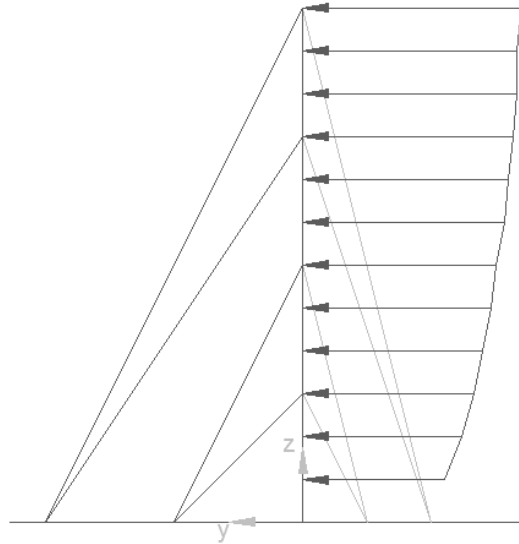


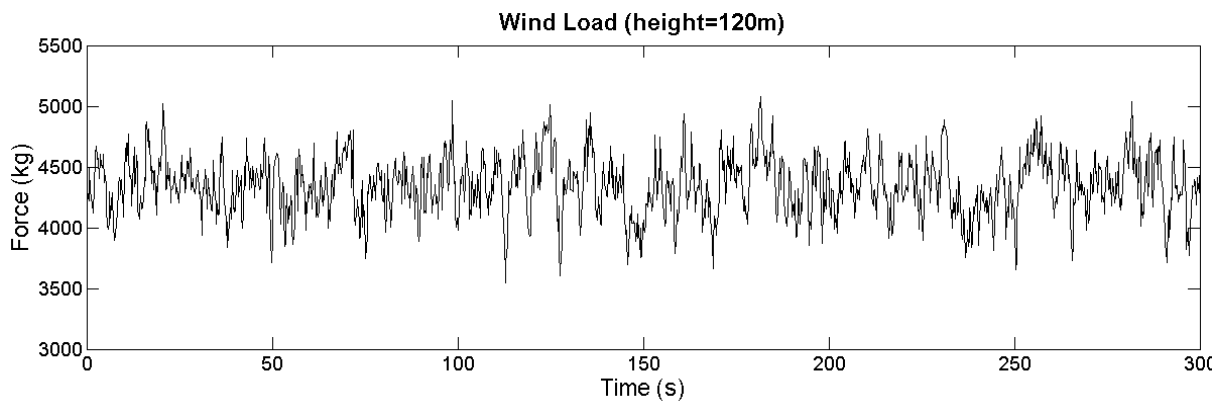Figure 4: Distribution of mean load along the height.



Figure 5: Wind load at 120 m.

## 4.2  Load Application

In this study, three loads were taken into account: gravity, pretension on the guys and the external excitation (wind). The pretension is applied at the beginning and holds during the whole calculus. This value is added or subtracted to the temporal variations of the tension due the external excitation. The gravity grows linearly from the beginning to the standard value in 3 s, and remains during the whole experiment. The wind load is applied starting at 4 s to the end of the calculus, to avoid the numerical instabilities due to the sudden application of pretension. Figure 6 illustrates the time application pattern of the loads.
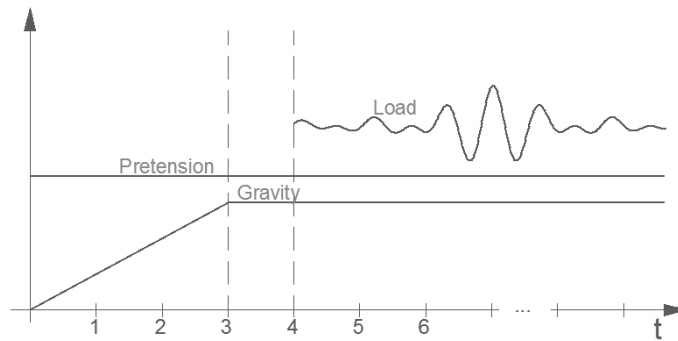


Figure 6: Temporal load application.

The total time of calculus was 300 s and the capture rate ($CR$) was of 5 frames per second, the same interval used to construct the wind load. Anyway, the time step is adaptive (it is adopted by the software in order to find convergence). The $CR$ may seem large, but the fundamental period of the mast is 2.66 s, then the adopted value provides an adequate precision to observe the dynamics of the problem.

## 5  WIND STUDY RESULTS

### 5.1  Displacements of the guyed mast

A typical displacement time history is showed in Fig. 7. For all the following analysis, the first 10 s were neglected, to avoid the effect of the abrupt application of the initial pretension and the wind load. All studied displacements are evaluated at the "y" direction (see Fig. 2) since this is the direction of the wind load and the directions along which the largest displacements occur.
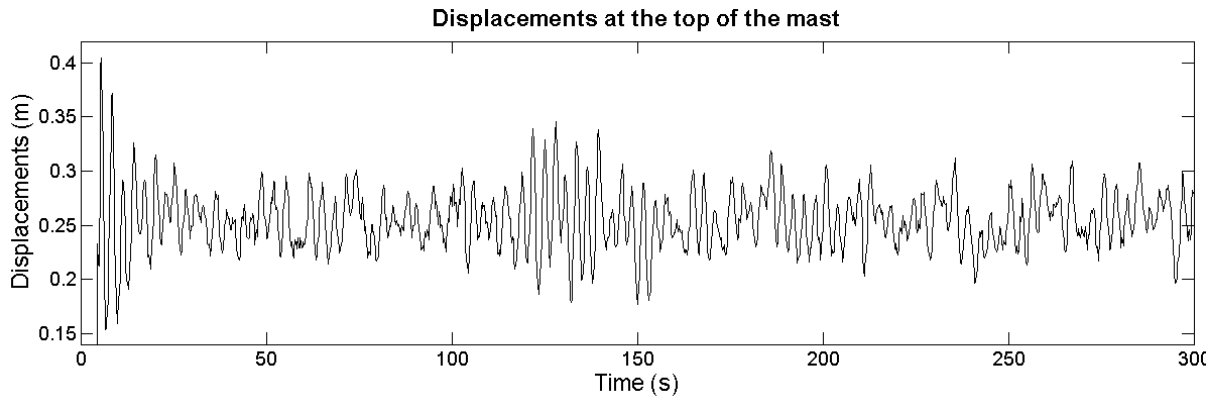
Figure 7: Displacement at 120 m. Time history.

The maximum displacement (MD) is one of the most important design variables related with the use of the guyed masts. A high quality transmission is not possible if large or non-admissible displacements are present. Since the antennas are usually located in the higher zone of the mast, the displacements produced in this part of the mast are of special interest. The displacements at 60, 70, 80, 90, 100, 110 and 120m (top of the mast) were analyzed.

Figure 8 shows the maximum displacements of the mast, obtained from the dynamic analysis, in three characteristic heights. The other cases are not shown for brevity, they simply describe intermediate states of the ones in Fig. 8. The results are ordered first by initial pretension case (IP), second by damping case (D) and finally by tower stiffness (TS), starting from the higher values. Then, the first mark (sort order 1) will be the case 35kN-3%-0.00270m$^4$ (IP-D-TS), the second mark (sort order 2) corresponds to 35kN-3%-0.00225m$^4$, the fourth mark (sort order 4) will be the case 35kN-2%-0.00270m$^4$ and so on. It can be noticed some kind of grouping of the maximum values of each studied case. However, the pattern changes with height. This indicates that the different variables (IP, D and TS) affect differently the MD with the height, but is still difficult to establish the influence of each distinct variable on the response.
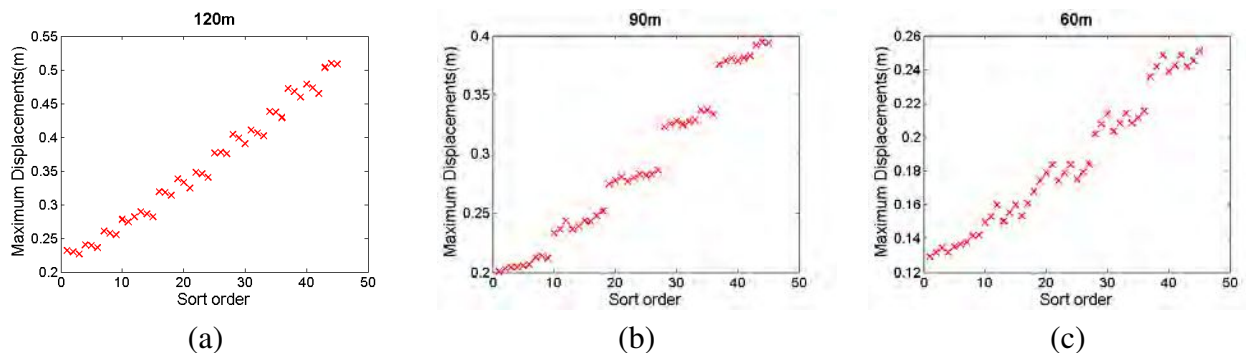


(a)

(b)

(c)

Figure 8: Maximum displacements for three different heights.

Basically, in order to identify how much the response changes or *varies* with the different values of some parameter, in other words, how big is the variation due to a given parameter, the *standard deviation will be used*. Figure 9 shows the standard deviations (SD) of the MD due to each parameter. To explain how the SD was computed, let us illustrate it by an example: the SD of the MD due the IP is sought, first the values due the combinations of the values of D and TS

-nine in total for each value of IP- should be averaged. These lead to five values (one for each value of IP) and the SD is computed over those values. Figure 9(a) depicts, with no doubt, that the IP is, by far, the parameter that generates the largest variation in the response. It does not mean that the D or TS have no influence on the response, it only fixes a scale of importance. It also explains why the MD, sorted as in Fig. 8 shows (globally) that for a higher sort order (or lower IP) higher values of MD are obtained.
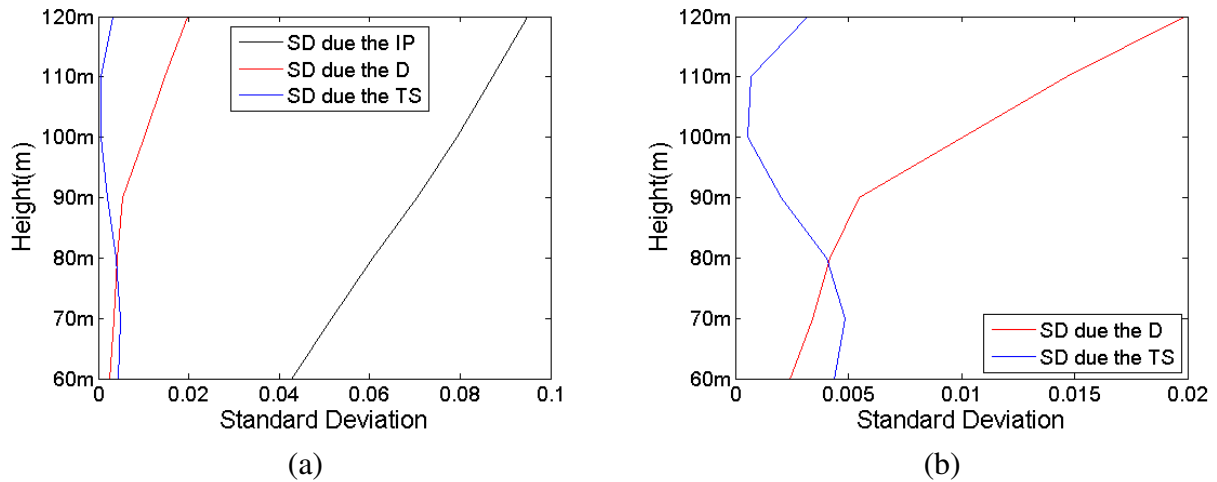


Figure 9: Standard deviations due the studied parameters.

Figure 9(b) shows an enlarged view of Fig. 9(a) for the range SD<0.02. It is observed that the importance of D and TS on the MD depends on the height and this result can explain the "grouping" seen in the Fig. 8(c) (MD at 60m height). TS has almost twice of importance than D for the MD (Fig. 9(b)): groups of three consecutive values can be immediately identified and they are almost parallel to other similar groups. Each one of these values corresponds, as explained before, to a singular value of TS and the group of three corresponds to a given value of D. The fact that the singular values are well separated justifies the importance of the TS. The parallelism among groups justifies the almost negligible influence of D. The opposite case can be seen in Fig. 8(a). Groups of three elements are apparent, though poorly separated (the influence of TS is negligible) and groups look, in general, like steps (the influence of the D is higher than the TS). An interesting fact in Fig. 8(a) is that higher values of TS give higher values of MD at the top of the mast (Fig. 8(a)), contrary to expectations.

The influence of a given parameter has also a complex dependency on the other parameter values. In other words, the deviation for the D, for example, depends on the height, as seen in Fig. 9 but also depends on IP and MS. Figure 10 is a mosaic diagram that illustrates this interdependency on the heights of 60m, 90m and 120m. The darker color implies that the, for the combination of the axes parameters, the studied variable generates very little variation (i.e. its influence on MD is poor), the lighter color implies the opposite. The light/dark colors are relative to the actual height (not to the absolute maximum SD) It can be seen that the "mean" color of each subfigure matches with the relation between D and TS in Fig. 9(b). It is possible to find some special cases, like the top figure in (c) that shows that D, for the 25kN case, and for any TS seems to have a negligible effect or, for the 35kN case in all scenarios of height and for any value of D, the TS has the minimum influence. But these are specific situations and the authors do not found a general trend or relationship.

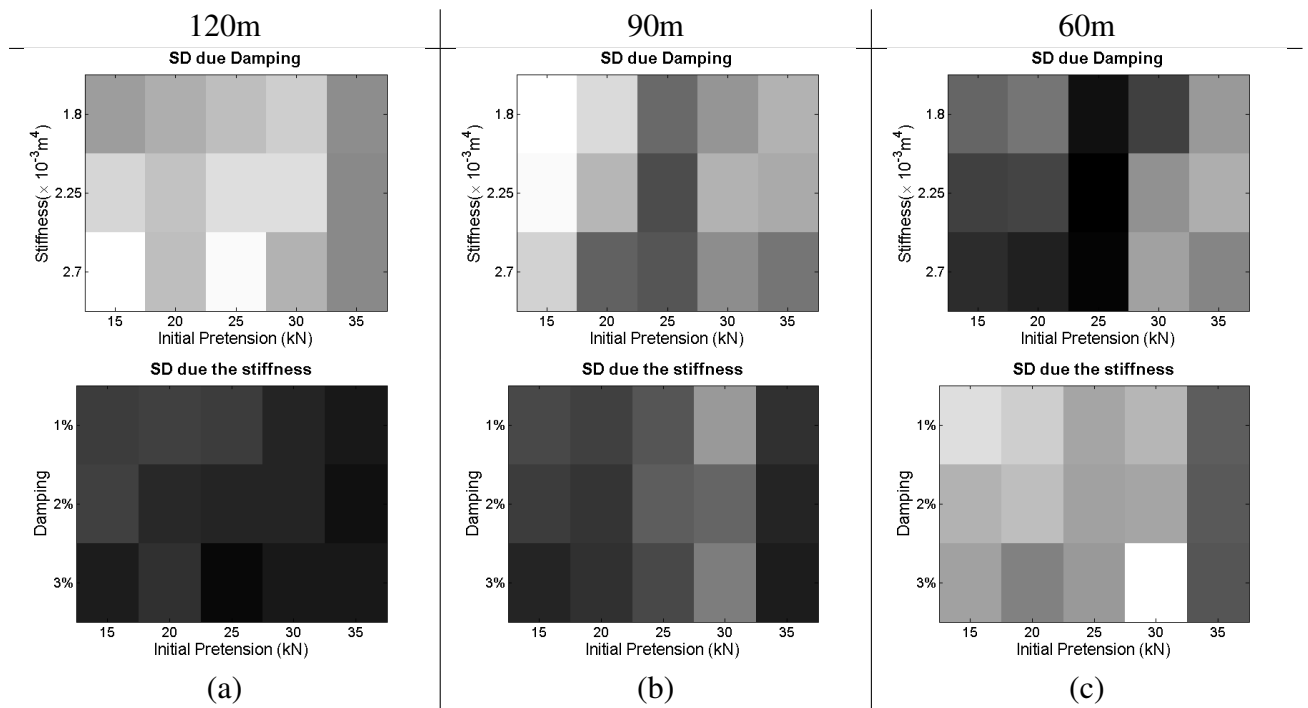|  |  |  |
|---|---|---|
| 120m | 90m | 60m |

Figure 10: Standard deviations. Complex interactions within parameters.

Finally, a comparison between the results of the MD at the top, obtained with the present study and the results of a previous work of the same authors (Ballaben et al. (2011)) is now discussed. In the latter study, the dynamics of the wind velocity was modeled as a superposition of cosine functions with frequencies extracted from the same spectrum used in here to reproduce the stochastic wind velocity field and the loads were fully correlated. Figure 11 is presented to illustrate the differences of the MD for the different types of load. The sorting of the values is the same as the used in the Fig. 8. Here, the 120 m MD is illustrated since the displacements for other heights exhibit similar fashion, in the case of the previous work. This fact in itself marks a first difference between the behaviors. The maximum values for de MD seems to be larger in Fig. 11(b), but the amplitude of the wind velocity field was set arbitrarily in that work. From Fig. 11(b) it also can be seen that the D is completely negligible and the TS produces always the same variation. Here, it seems that the parameters have an independent behavior. The obvious common point is that the IP is the most influent variable.

The behavior of the case studied in Ballaben et al. (2011) is associated with the load. It was used the same psdf and a cosine superposition, but the frequencies selected were equally spaced, and the final load only employees 10 frequencies. Thus the obtained load was harmonic, and the frequencies combined were low, extracted from the peak zone of the psdf of Davenport. Then, the displacements history, at any point of the height and for any combination of parameters, almost copy the curve of the loads, as can be seen in Fig. 12, due the loads were quasi-static. The method used in the present work uses all the range of frequencies of the spectrum, allowing to model the dynamics of the wind velocity field with more detail, taking into account the temporal and spatial correlations and permitting a better understanding of the dynamic behavior of the guyed masts.

A Fast Fourier Transform (FFT) study was also performed for the displacements. Figure 13 shows the FFT of the displacements for the standard case 25kN-2%-0.00180m$^4$ (IP-D-TS) for the top of the mast, and the corresponding theoretical spectrum. Similar results are found when
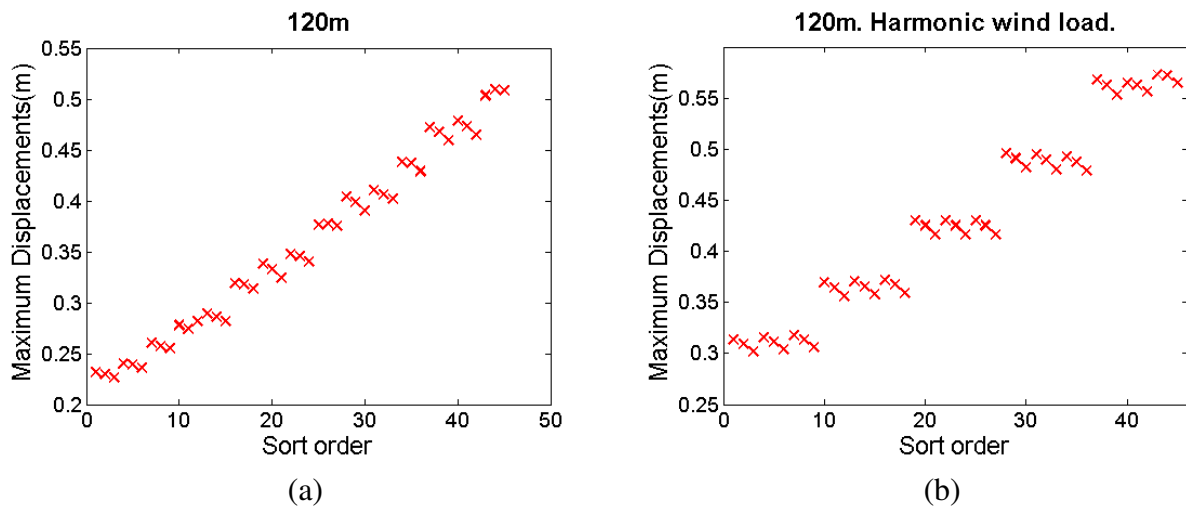
Figure 11: Comparison between maximum displacements for a wind load generated (a) by a stochastic wind velocity field (b) by a harmonic wind velocity field.
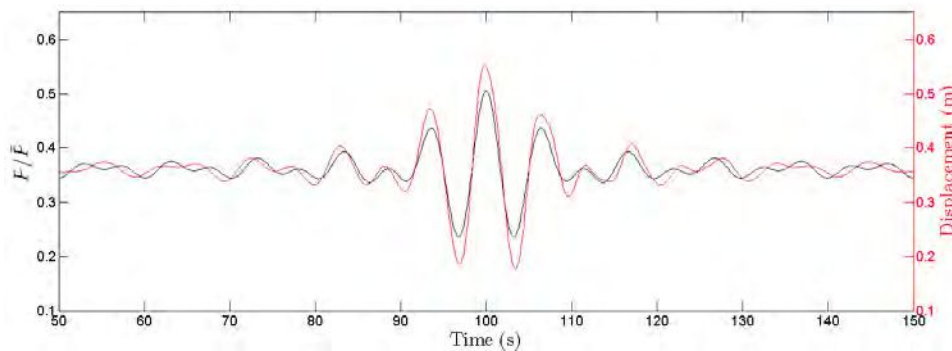


Figure 12: Typical displacement diagram for the harmonic load.

the displacements are analyzed for other parameter values or for other heights. The spectrum of the displacements do not match with the spectrum of the loads. In opposition, the spectrum of the displacements in Ballaben et al. (2011), matches closely with the spectrum of the loads and can be appreciated the decrease of the energy when compared low values of IP with high values of IP (Fig. 14).

## 5.2 Tension on Guys

The tension on guys is an important design variable, since the anchor points of the guys are support points that divide the mast length in segments to reduce the buckling risk and give more stiffness at the structure. Then, it is important to know the variation of the guy tension during the dynamic event.

Figure 15 illustrates the maximum guy tension (MA) in red, the mean guy tension (ME) in black and the minimum guy tension (MI) in blue, for the level 2 of the "b" direction (see Figure 2). The values are sorted in the same way as in Fig. 8 (i.e. first by IP, then by D and then by TS), but starting from the lower values of the parameters, instead of the highest. In Fig. 15(a) the results are expressed as a percentage of the IP and in Fig. 15(b) as absolute values.

Figure 15(a) depicts the result for the "'b2" cable, and it is reported here to show the highest MA values. The highest mark exceeds the 240% of IP, for 15kN case of IP. When the IP values
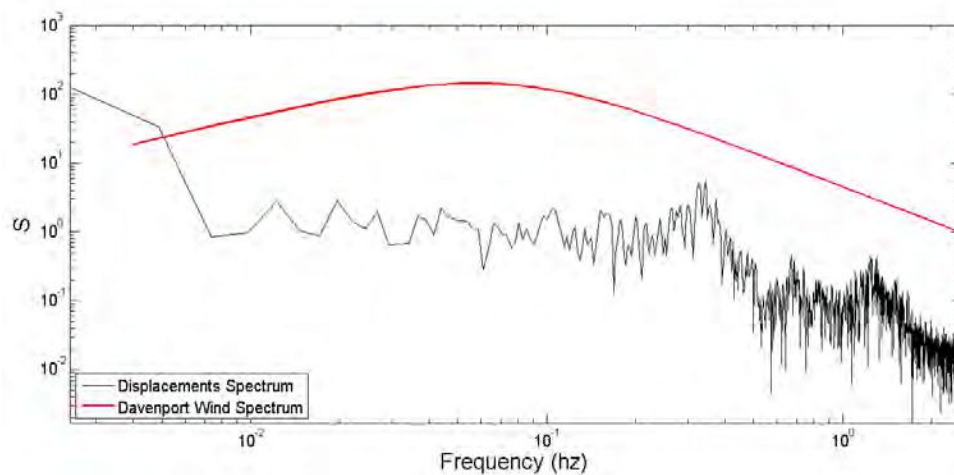
Figure 13: Comparison of the FFT of the displacements at the top, for the standard case (25kN-2%-0.00180m$^4$) with the theoretical psdf of the wind loads.
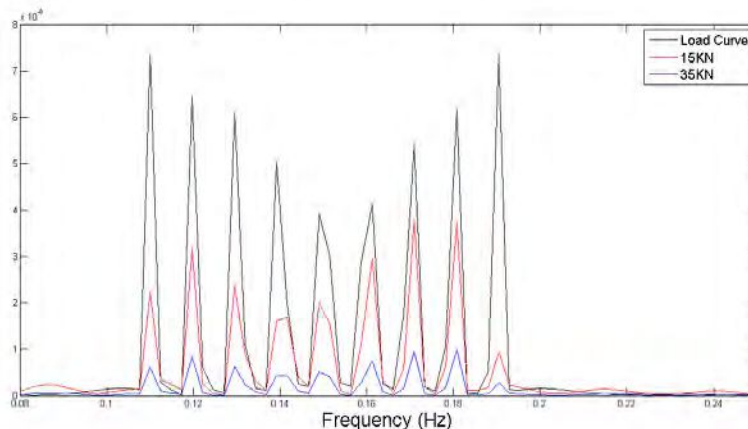


Figure 14: FFT analysis of the displacements at the top for the harmonic load.

increase, all the MA, ME and MI (in % of IP) values diminish and the differences between MA and MI become lower; this trend exhibits large changes when the lower three values of IP are observed and then continues, but with much lower influence. The difference between MA and MI is about 60% of IP in the 15kN case and descends to no more than the 15% for the 35kN case. Figure 15 (b) illustrates the MA, ME and MI absolute values of guy tension. The guy tension (MA, ME, and MI) rises when IP increases, but the increment related to the IP become lower while higher values of IP are studied. Other levels of cables in "b" direction are not showed because they exhibit similar behaviors.

MA, ME and MI guy tension are shown in Fig. 16, as a percentage of IP, for the cables at levels 3 and 4 in the "a" direction. The sort and color scale are the same as in Fig. 15. Figure 16 (a) is presented here to depict the absolute minimum of the tension of all guys, and shows that even the loosest guy never loses all the IP. Figure 16(a) also shows that the MA, ME and Mi values decrease with increasing IP with a minimum in 30kN, where seems that the trend reverts. Figure 16(b) has a clearer minimum at 20kN. As can be observed in Fig. 16 the difference between MA and MI is poorly influenced by the IP.

In reference to the previous work, with a harmonic load, a similar behavior is observed for the
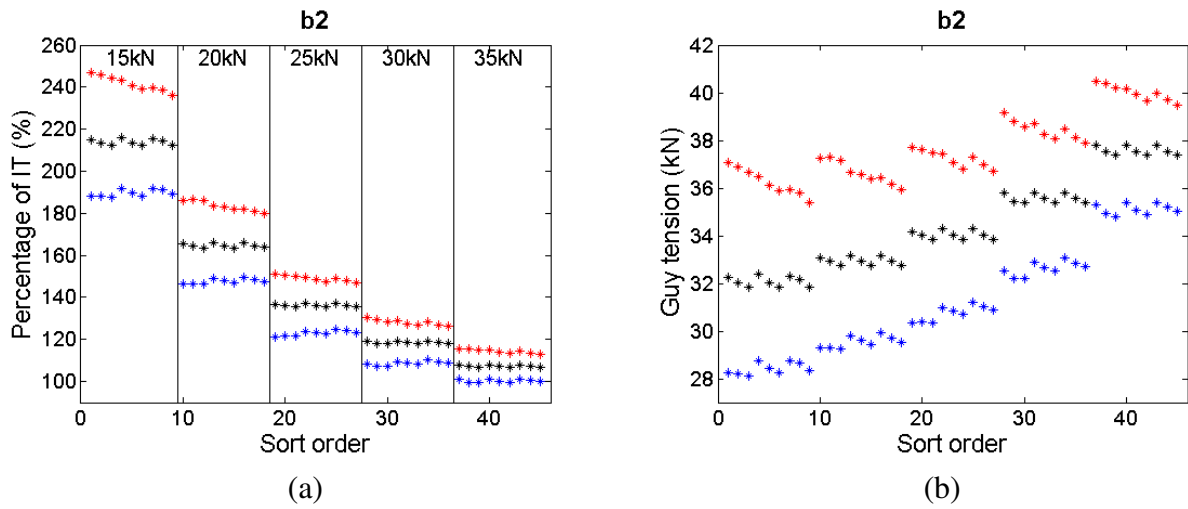
Figure 15: Maximum, mean and minimum tension for the guys at level 2 and "b" direction.

MA, ME and MI guy tension. In the present work, a larger influence of the TS and D on the guy tension i s observed. These influences are not studied in detail here because in guyed towers, they are not variables of interest (i.e. if the maximum stress of a guy exceeds the allowable value, the criterion indicates change the cable cross-section, not to increase the rigidity of the mast.).
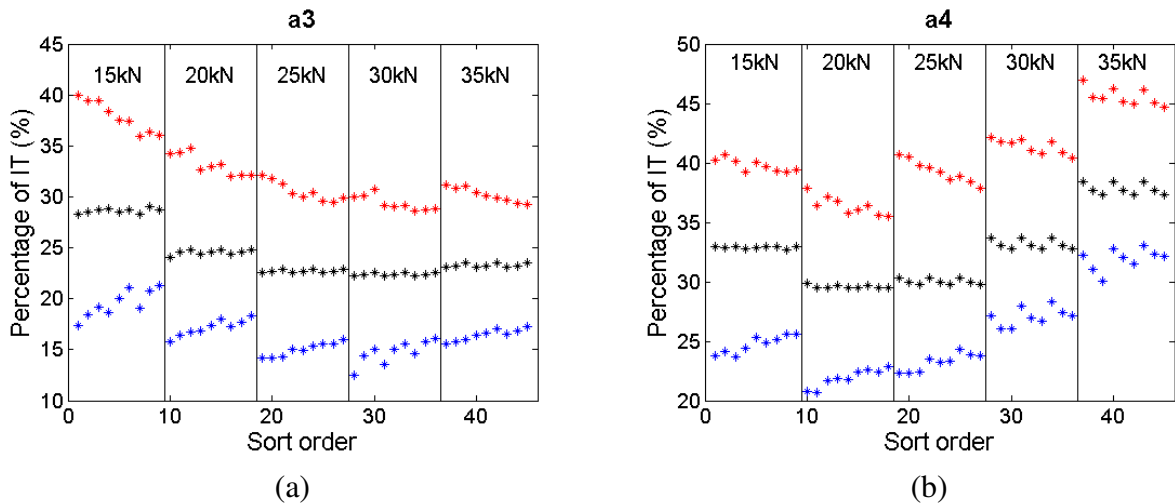


Figure 16: Maximum, mean and minimum tension for the guys at level a and "a" direction.

## 6 FINAL REMARKS

In this work a dynamic, non-linear finite element analysis of a guyed mast was carried out. The aim was to analyze the influence of pretension of the guys, the damping and the tower stiffness on the response of the system under a dynamic wind load derived from a stochastic wind velocity field that takes into account temporal and spatial correlations. The process to obtain the velocity field is carried out by means of the Spectral Representation Method (SRM) and it is explained in detail. The presented results were compared with the results of a previous work of the same authors where the load was dynamic, but constructed as a simple superposition

of cosine functions, with frequencies within the peak zone of the selected power spectrum density function.

The analysis of the displacements of the mast shows that the most influential variable for the maximum displacements is the initial pretension of the guys. The influence of the tower stiffness and damping is also remarkable, but to a much lesser extent. The importance of the damping and the tower stiffness was evaluated at different points of the height, finding that the impact of each parameter is highly dependent on the height. Also the complex interdependence between parameters is presented; the authors do not find any trend in this issue. The importance and variability of the influence of the damping and the tower stiffness on the displacements represent the major difference with the previous work. A remarkable but non expected engineering result is that an increase of the tower stiffness, leads to higher displacements at the top; the same trend was found in the previous work.

A FFT study was carried out as well. It was found that the FFT for different heights and parameter combinations has similar shapes and energy content and do not match with the theoretical power spectrum expression of the wind load. In opposition, in the previous work the match was perfect, and a large difference of energy can be found for different values for initial pretension. The study on the guy dynamic tension reveals that the maximum overstress rounds the 250% for the case of 15kN of initial prestress and the minimum tension of loosest cable has about the 10% of the initial prestress. The difference between maximum and minimum values of each case of pretension tends to decrease when increasing the initial pretension, for the more taut cables in the "b" direction. In the previous work, a similar behavior was found.

## REFERENCES

ALGOR. *ALGOR V23.01. Professional MES*, 2009.

ANSI/TIA-222-G. *Structural Standard for Antenna Supporting Structures and Antennas, ANSI/TIA-222-G*. Telecommunications Industry Association, 2009.

Ballaben J., Guzman M., and Rosales M. Parametric studies of guyed towers under wind and seismic loads. *Asociación Argentina de Mecánica Computacional*, 30:1019–1032, 2011.

CIRSOC-INTI. *Reglamento CIRSOC 102. Acción del Viento sobre las Construcciones* . INTI, Buenos Aires, Argentina, 2005.

CIRSOC-INTI. *Proyecto de Reglamento Argentino para Construcciones Sismorresistentes Parte 1. Construcciones en General*. INTI, Buenos Aires, Argentina, 2008.

de Oliveira M.I., da Silva J.G., da S. Vellasco P.C., de Andrade S.A., and de Lima L.R. Structural analysis of guyed steel telecommunication towers for radio antennas. *J. of the Braz. Soc. of Mech. Sci. and Eng.*, 29:185–195, 2007.

Dyrbye C. and Hansen S. *Wind Loads On Structures*. John Willey and Sons, West Sussex, England, 1 edition, 1994.

Gomathinayagam P.H.A.A.S. and Lakshmanan N. Full scale measurements of the structural response of a 50 m guyed mast under wind loading. *Engineering Structures*, 25:859–867, 2003.

Horr A.M. Nonlinear spectral dynamic analysis of guyed towers: Part i: Theory. *Canadian Journal of Civil Engineering*, 31:1051–1060, 2004.

IASS. *International Association for Shell and Spatial Structures*. IASS, Madrid, España, 1991.

Kahla N.B. Equivalent beam-column analysis of guyed towers. *Computers and Structures*, 55(4):631–645, 1993.

Kahla N.B. Response of a guyed tower to a guy rupture under no wind pressure. *Engineering Structures*, 22:699–706, 2000.

Kewaisy T.H. *Nonlinear Dynamic Interaction between Cables and Mast of Guyed-Tower Systems Subjected To Wind-Induced Forces*. Ph.D. thesis, Texas Tech University, 2001.

Lu L., Qu W., and Li M. Simulation of wind velocity and calculation of wind load for guyed masts. *Wuhan Ligong Daxue Xuebao (Jiaotong Kexue Yu Gongcheng Ban)/Journal of Wuhan University of Technology (Transportation Science and Engineering)*, 34:1057–1060, 2010.

Matuszkiewicz M. Calculation of guyed masts in accordance with en 1993-3-1 standard taking into account mast shaft geometrical imperfections. *Engineering Structures*, 33:2044–2048, 2011.

Meshmesha H., Sennah K., and Kennedy J.B. Simple method for static and dynamic analyses of guyed towers. *Structural Engineering and Mechanics*, 23(6):635–649, 2006.

Preidikman S., Massa J., and Roccia B. Análisis dinámico de mástiles arriostrados. *Rev. Int. de Desastres Naturales, Accidentes e Infraestructura Civil*, 6(1):85–102, 2006.

Punde Y.D.S. Simple model for dynamic analysis of cable supported structures. *Engineering Structures*, 23:271–279, 2001.

Shi H. *Nonlinear Finite Element Modeling and Characterization of Guyed Towers Under Severe Loading*. Ph.D. thesis, University of Missouri, Columbia, 2007.

Shinozuka M. and Jan C.. Digital simulation of random processes and its applications. *Journal of Sound and Vibration*, 25(1):111–128, 1972.

Wahba M., Madugula M., and Monforton G. Evaluation of non-linear analysis of guyed antenna towers. *Computers and Structures*, 68:207–212, 1998.

Wahba M.M.Y. and Monforton G. Dynamic response of guyed masts. *Engineering Structures*, 20(12):1097–1101, 1998.